

Yoshihiro Wakayama · Masahiko Inoue ·  
Hiroko Kojima · Takahiro Jimi · Seiji Shibuya ·  
Hajime Hara · Hiroaki Oniki

## Expression and localization of aquaporin 7 in normal skeletal myofiber

Received: 6 May 2003 / Accepted: 13 January 2004 / Published online: 17 February 2004  
© Springer-Verlag 2004

**Abstract** We examined whether AQP7 molecules are expressed in the normal skeletal muscle at mRNA and protein levels. Gel electrophoresis of the reverse transcription-polymerase chain reaction (RT-PCR) product of total RNA samples of normal human or mouse muscles by using oligonucleotide primers for human or mouse AQP7 showed a band of 328 or 369 basepairs, which corresponded to the basepair length between two primers of AQP7. The nucleotide sequence of these RT-PCR products coincided with those of human and mouse AQP7. Immunoblot, immunohistochemical and immunoelectron-microscopic studies of the protein were done by using the rabbit antibody against the synthetic peptide of the N-terminal cytoplasmic domain of the human AQP7 molecule. Immunoblot analysis showed that the rabbit antibody against human AQP7 reacted with a protein of approximately 30 kDa molecular weight in extracts of normal human and mouse skeletal muscles, and normal mouse liver. Immunohistochemistry with our anti-AQP7 antibody showed an immunoreaction at the myofiber surface of type 1 and type 2 fibers in human muscles and of type 2 fibers in mouse muscles.

**Keywords** Aquaporin 7 · Normal skeletal myofiber · Localization · Human · Mouse (C57BL/10ScSn)

### Introduction

Aquaporins (AQPs) are channel-forming integral membrane proteins that serve as selective pathways to facilitate water transport across plasma membranes of many tissues and cell types. In the last decade, genes for several AQPs have been cloned, and more than ten AQPs have so far been identified from mammalian tissues. Among them, AQP3, 7, 9 and 10 are functionally and structurally unique (Ishibashi et al. 1998; Hatakeyama et al. 2001). Functionally they transport non-ionic small molecules, such as glycerol and urea, in addition to water, but other AQPs, such as AQP1, 2, 4, 5 and 8, transport only water.

The water permeability of mammalian AQP molecules, except for AQP4 and 7, is inhibited by mercury chloride (Shi and Verkman 1996; Ishibashi et al. 1997). Mercury-sensitive Cys is just in front of the second 3-amino-acid residue NPA motifs (Asn-Pro-Ala) in AQP1, 2, 5, 6, 8 and 10, showing that this is a functionally important region of the protein (Preston et al. 1993; Koyama et al. 1998). Although AQP9 molecules are also mercurial sensitive, they have no such mercury inhibitory Cys residue site (Kuriyama et al. 1997). AQP4 and 7 are insensitive to mercury chloride and they have no such Cys in their amino acid sequences (Ishibashi et al. 1997). Three Cys are present in the deduced amino acid sequence of AQP7, but they are not near the second NPA motif and they may not be localized near the AQP7 aqueous pore (Ishibashi et al. 1997).

AQP4 in skeletal muscle has been extensively studied (Frigeri et al. 1998, 2001, 2002; Liu et al. 1999; Jimi et al. 2000; Wakayama et al. 2001, 2002a). The reduced expression of AQP4 in the muscles of boys with Duchenne dystrophy (Frigeri et al. 2002; Wakayama et al. 2002a) and of mdx mice (Liu et al. 1999; Frigeri et al. 2001; Crosbie et al. 2002) has been described. Several investigations have been reported on other AQPs. AQP1, 3 and 4 mRNAs are expressed in normal rat skeletal muscle (Umenishi et al. 1996); we recently found the expression and localization of AQP3 in normal human skeletal myofibers (Wakayama et al. 2002b). AQP5 is

Y. Wakayama (✉) · M. Inoue · H. Kojima · T. Jimi · S. Shibuya · H. Hara  
Department of Neurology,  
Showa University Fujigaoka Hospital,  
1-30 Fujigaoka, Aoba-Ku, 227-8501, Yokohama, Japan  
e-mail: wakayama@showa-university-fujigaoka.gr.jp  
Tel.: +81-45-9711151  
Fax: +81-45-9742204

H. Oniki  
Electron Microscope Laboratory,  
Showa University Fujigaoka Hospital,  
Yokohama, Japan

expressed in regenerating skeletal muscle (Hwang et al. 2002). A reverse transcription-polymerase chain reaction (RT-PCR) study using mRNAs from the mouse extensor digitorum longus and soleus muscles with a positive control found strong bands of AQP1 and 4 and weak bands of AQP7 and 9 (Yang et al. 2000).

In this study, we investigated the expression and localization of AQP7 in normal human and mouse skeletal myofibers at mRNA and protein levels.

## Materials and methods

### Muscle samples

Six histologically and histochemically normal quadriceps femoris muscle samples were obtained under local anesthesia from patients who were thought to have myopathy but were judged to be free of neuromuscular disorders after histochemical and immunologic examinations and who gave informed consent. Muscle samples were obtained by procedures approved by the Human Ethics Committee of Showa University. Six normal mice (C57BL/10ScSn) were killed by cervical dislocation and the quadriceps femoris muscles and livers were excised.

### Reverse transcription-polymerase chain reaction (RT-PCR)

Total RNA was extracted from approximately 30 mg of each normal human or mouse muscle, or mouse liver sample with an acid phenol extraction reagent (TRIZOL, Gibco BRL, Rockville, MD). AQP7 mRNA was detected by RT-PCR. Oligonucleotide primers were designed from human AQP7 sequences (Ishibashi et al. 1998; Entrez NM001170), sense strand (hAQP7F) 5'-GAG-GAAGATGGTGCGAGAG-3', and antisense strand (hAQP7R) 5'-GAGAATGGCCGTGTAGAAGAG-3'. Primers were also designed from mouse AQP7 sequences (Entrez BC022223), sense strand (mAQP7F) 5'-TGGGTTTTGGATTCCGGAGT-3', and antisense strand (mAQP7R) 5'-TGTTCTTCTGTGCGGTGATGG-3'. Both RT-positive (RT+, addition of reverse transcriptase) and RT-negative (RT-, no addition of reverse transcriptase) experiments were done. Total RNAs from human and mouse muscles were reverse transcribed for 30 min at 50°C, and then at 35 cycles of PCR (30 s each at 85°C and 60°C and 1 min at 72°C) for human RNA and (30 s each at 85°C and 52°C and 1 min at 72°C) for mouse RNA. The reaction mixture contained 1×PCR buffer, 2 μM of each primer pair, 5 mM magnesium chloride, 1 mM of each dNTP analogue mixture, 0.8 U/μl ribonuclease inhibitor, 0.1 U/μl Taq polymerase, and 0.1 U/μl reverse transcriptase in the RT-positive experiment [mRNA selective PCR kit (code RR025A); TaKaRa Co.]. In the same mixture, reverse transcriptase was not added in the RT-negative experiment. As positive control, total RNA from normal human liver (OriGene Technologies, Rockville, MD) and mouse liver was amplified in the same way by RT-PCR. The RT-PCR products were observed by means of 2% agarose gel electrophoresis. The nucleotide sequences of the main band of RT-PCR products of total RNAs from normal human and mouse skeletal muscle were analyzed to confirm whether the band was AQP7.

### Peptide synthesis of AQP7 and antibody production

General procedures for peptide synthesis and antibody generation were similar to those described previously (Wakayama et al. 1990). Briefly, the peptide (MVQASGHRSTRGSK-C) of the N-terminal end of the cytoplasmic domain in the human AQP7 molecule (Entrez NM001170) was synthesized and extra cysteine was added to the C-terminus of this peptide. Bovine thyroglobulin was added

at an extra cysteine residue (Peptide Institute, Inc., Osaka, Japan). The antibody against this peptide was generated in rabbits. Solid-phase enzyme-linked immunosorbent assay was used to find the rabbit polyclonal antibody titer, which was ×102,400. This antiserum was affinity purified.

### Immunoblot analysis of the antibody

Immunoblot analysis of the antibody against AQP7 in histochemically normal specimens of human and mouse quadriceps femoris muscles and normal mouse livers was done by using a previously described method (Wakayama et al. 2002b) with minor modifications. Sodium dodecyl sulfate polyacrylamide gel electrophoresis was performed with a 12.5% homogeneous gel for AQP7. The protein was transferred from the gel to a clear blot P membrane sheet (ATTO, Tokyo, Japan) by horizontal electrophoresis at 108 mA for 90 min at room temperature. Immunostaining was done with affinity-purified rabbit anti-AQP7 antibody solution and an immunodepleted antibody solution that was preincubated with the excess amount of the synthetic peptide antigen of AQP7.

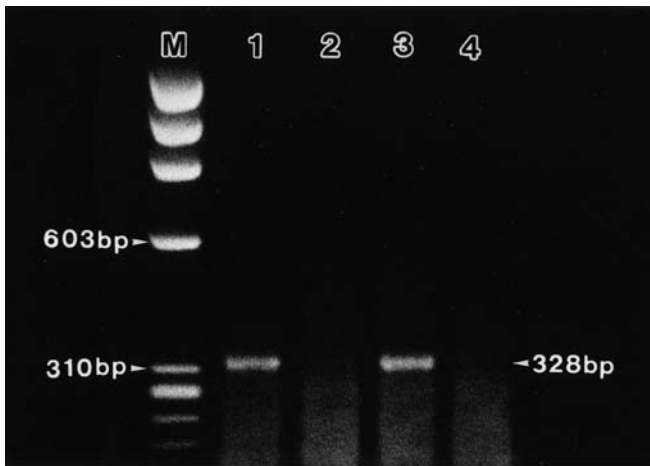
### Immunohistochemistry

Human and mouse muscle samples and mouse liver specimens were immediately frozen in isopentane cooled with liquid nitrogen. Frozen 6-μm-thick cross sections of the muscle and liver samples were placed on coverslips and were incubated with affinity-purified primary rabbit anti-AQP7 antibody diluted to a final IgG concentration of 5 μg/ml. The negative control specimens were prepared by using the preimmune serum and the immunodepleted antibody solution; the latter was prepared by preincubation of the anti-AQP7 antibody solution with an excess amount of AQP7 peptide antigen. To test the cross-reactivity of our anti-AQP7 antibody with other AQPs in skeletal muscle, the preincubated solution of the anti-AQP7 antibody with an excess amount of AQP3 and AQP4 peptide antigens was prepared and was used with the muscle and liver specimens. Indirect immunofluorescent staining was done by a method previously described (Wakayama et al. 2002b). Serial sections were immunostained with the rabbit anti-AQP4 antibody that was described previously (Wakayama et al. 2002b). Immunogold electron microscopy was also performed by using six normal human quadriceps femoris muscles in order to examine the ultrastructural localization of AQP7. General procedures were similar to those described previously (Wakayama et al. 2002b).

## Results

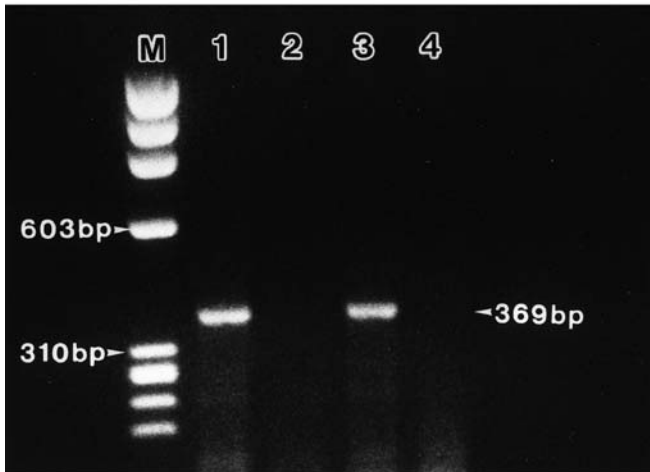
### RT-PCR

Gel electrophoresis of the AQP7 RT-PCR products of the total RNAs from normal human and mouse muscles showed a single band of 328 basepairs (Fig. 1A, lane 1) and 369 basepairs (Fig. 1B, lane 1) in the RT-positive experiment, but showed no band (Fig. 1A, lane 2, B, lane 2) in the RT-negative experiment. Analysis of the nucleotide sequence of RT-PCR products of human and mouse skeletal muscle RNAs in the RT-positive experiment showed that the sequence coincided with the human and mouse AQP7 sequence between the sense and antisense primers. Gel electrophoresis of the AQP7 RT-PCR products of human and mouse liver RNAs showed a single band of 328 basepairs (Fig. 1A, lane 3) and 369 basepairs (Fig. 1B, lane 3) in the RT-positive



**A**

	+	-	+	-	RT
	Human Skeletal Muscle		Human Liver		



**B**

	+	-	+	-	RT
	Mouse Skeletal Muscle		Mouse Liver		

**Fig. 1** Gel electrophoresis of the reverse transcription-polymerase chain reaction (RT-PCR) product of total RNA from normal human (**A**) and mouse (**B**) skeletal muscles using the primers for human and mouse aquaporin 7 (AQP7). The products contained a single band of 328 and 369 basepairs, respectively, in the RT-positive experiment (**A, B, lane 1**), but that in the RT-negative experiment contained no bands (**A, B, lane 2**). Gel electrophoresis of the AQP7 RT-PCR product of human and mouse normal liver RNAs showed a single band with 328 and 369 basepairs in the RT-positive experiment (**A, B, lane 3**), respectively, but that in the RT-negative experiment contained no band (**A, B, lane 4**). Lane M is  $\times 174$  HaeIII digest marker

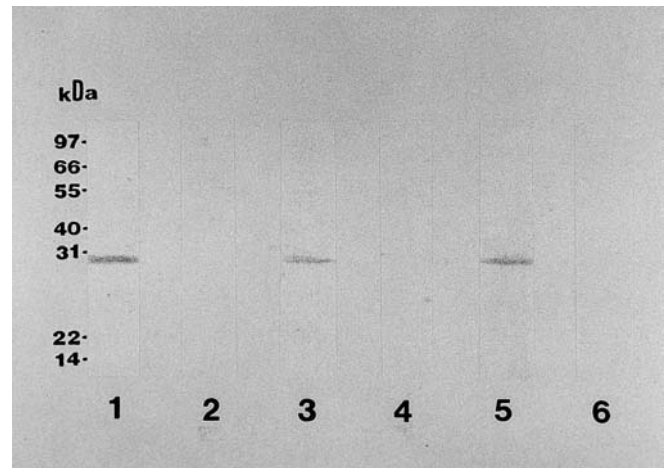


**Fig. 2** Immunoblot analysis showed that our affinity-purified rabbit anti-aquaporin 7 antibody reacted with a protein of approximately 30 kDa molecular weight in normal human (*lane 1*) and mouse (*lane 3*) skeletal muscle extracts and in normal mouse liver (*lane 5*), but immunoblot analysis using the immunodepleted antibody solution did not show this band (*lanes 2, 4, 6*). Numbers to the left indicate the molecular masses of standards

experiment, but showed no band (Fig. 1A, lane 4, B, lane 4) in the RT-negative experiment.

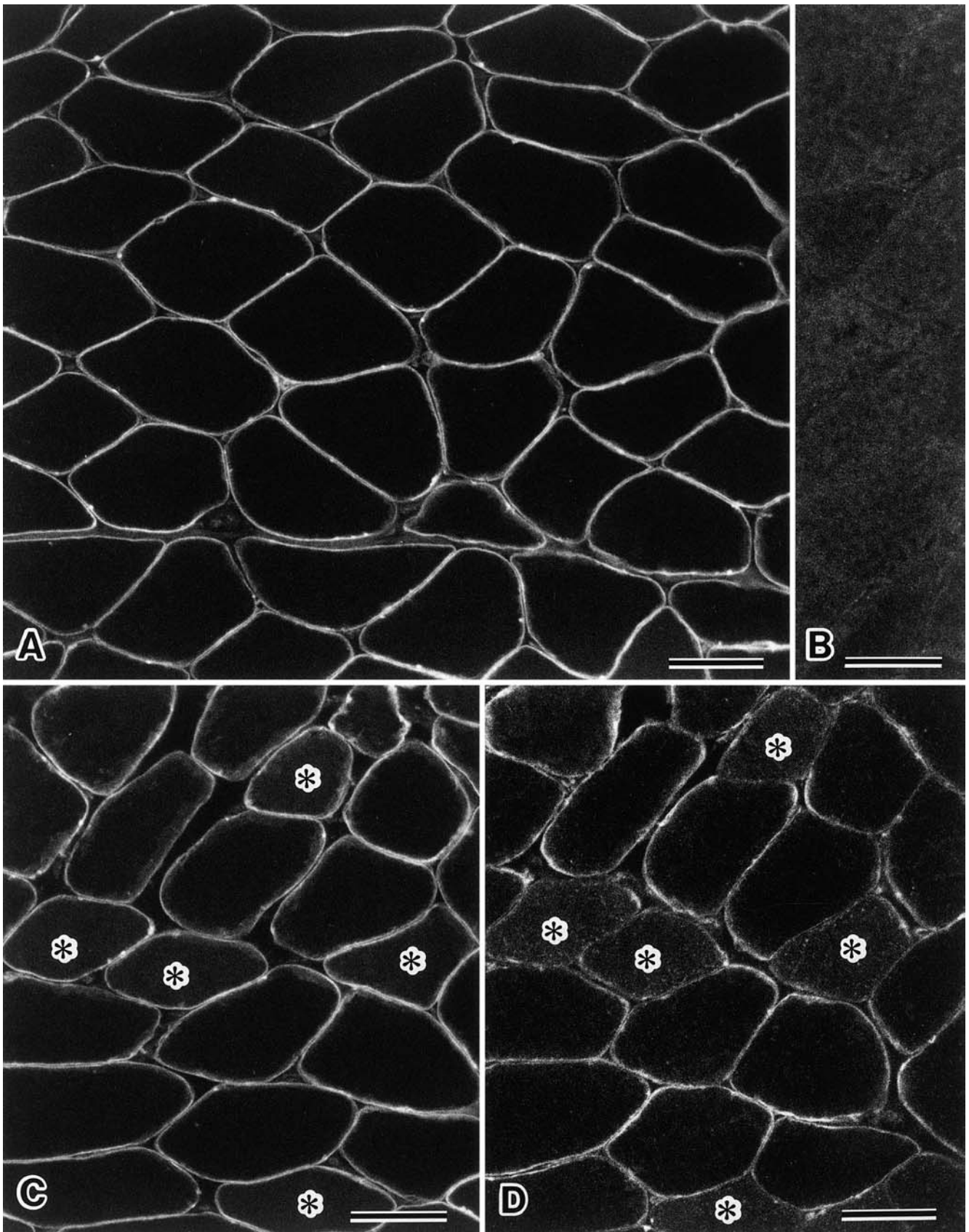
#### Immunoblot analysis of the antibody

Immunoblot analysis showed that the affinity-purified rabbit antibody against the synthetic peptide of the N-terminal end of the cytoplasmic domain of human AQP7 molecule reacted with a protein of approximately 30 kDa molecular weight in the extracts of human and mouse quadriceps femoris muscles (Fig. 2, lanes 1, 3) and mouse liver (Fig. 2, lane 5). However, immunoblot analysis using the immunodepleted antibody solution showed no band (Fig. 2, lanes 2, 4, 6).

#### Immunohistochemistry

Immunohistochemistry showed that the rabbit polyclonal antibody against AQP7 clearly stained the surface of cross sections of normal human skeletal myofibers. Both type 1 and type 2 myofibers were stained and the staining pattern appeared to be continuous by light microscopy and no intracellular structures were stained (Fig. 3A). The myofibers immunostained with the preimmune rabbit serum or the immunodepleted antibody solution showed no immunostaining (Fig. 3B). The difference between myofiber types in the immunoreactivity of our anti-AQP7 antibody was not definite (Fig. 3C) compared with that of the anti-AQP4 antibody seen in the serial sections of the human muscle tissue (Fig. 3D). In contrast, immunohistochemistry with our anti-AQP7 antibody in normal mouse skeletal muscle showed a positive immunoreaction at the cell surface of the cross sections of myofibers and





the immunostaining pattern appeared to be discontinuous. The distribution of mouse skeletal myofibers with a positive AQP7 immunoreaction showed a checkerboard pattern (Fig. 4A, B). Positively stained mouse myofibers with our anti-AQP7 antibody were also strongly stained with the anti-AQP4 antibody in the serial sections of mouse muscle tissue (Fig. 4C). Sections of mouse liver showed positive immunostaining with the anti-AQP7 antibody at the hepatocyte periphery (Fig. 4D). The immunoreactivity of the preincubated anti-AQP7 antibody solution with excess amounts of AQP3 and AQP4 peptide antigens was positive in the sections of human and mouse skeletal myofibers. Single immunogold-labeled electron microscopy of normal human muscle samples immunostained with rabbit anti-AQP7 antibody showed 5-nm gold particles along the muscle plasma membrane.

## Discussion

AQP families of proteins are integral membrane proteins that are predicted to contain six transmembrane domains. The N- and C-termini are predicted to be cytoplasmic. These integral membrane proteins are visible by freeze-fracture electron microscopy, because the fracture plane preferentially goes to the hydrophobic interior of the biological membrane and yields two leaflets of the protoplasmic (P) face and the extracellular (E) face. For example, freeze-fracture electron microscopy shows the P face of the normal skeletal muscle plasma membrane that contains an orthogonal array assembly of more than four approximately 6-nm-diameter particles. This assembly is composed of AQP4 (Yang et al. 1996). The muscle plasma membrane P face of a freeze-fracture replica contains numerous intramembranous particles of various diameters, the function of which are mostly unknown. We were interested in the functional roles of the intramembranous particles and thought that classes of AQPs other than AQP3 (van Hoek et al. 1998) and AQP4 might exist in the plasma membrane of skeletal muscle.

This investigation of the RNA and protein showed that the plasma membrane of the normal human skeletal muscle contained AQP7 in addition to AQP3 and 4. The AQP4 molecules are more abundantly expressed in fast-twitch type 2 myofibers (Frigeri et al. 1998), but the AQP3

molecules are more intensely expressed in slow-twitch human type 1 muscle fibers (Wakayama et al. 2002b). AQP7 is strongly expressed both in slow-twitch type 1 myofibers and in fast-twitch type 2 myofibers in human skeletal muscles, but it is almost exclusively expressed in type 2 myofibers of mouse skeletal muscles. In this study, the cell surface showed an apparent difference in immunostaining pattern with our anti-AQP7 antibody between the cross-sectioned human and mouse myofibers: human myofibers showed a continuous staining pattern but mouse myofibers showed a discontinuous pattern. The reason for this difference is unknown, but possible explanations include: (1) a difference in species and (2) the characteristics of our antibody that was generated against the human AQP7 synthetic peptide. AQP3, 7 and 9 are functionally and structurally similar except that AQP7 is insensitive to mercury chloride, unlike AQP9. The AQP4 molecule permeates the water molecule alone (Hasegawa et al. 1994), but AQP7 and 3 molecules function as a channel of glycerol and urea, as well as water (Ishibashi et al. 1994; Inase et al. 1995). In mammals, AQP3 has long been cloned from rat sperm that also facilitates glycerol permeation. The strong immunoreactivity of anti-AQP7 antibody in both human myofiber types and an almost exclusive AQP7 immunoreactivity in type 2 mouse myofibers may imply the need for this channel for their metabolism. We believe that our anti-AQP7 antibody really recognized the AQP7 molecule for the following reasons: (1) the synthetic peptide of the N-terminal domain of human AQP7 showed no homology with other AQPs and (2) the preincubated anti-AQP7 antibody solution with excess AQP3 and 4 synthetic peptide antigens showed a positive immunoreactivity in human and mouse myofibers.

To explore further functional roles of AQP7 in skeletal muscles, studies on the following issues may be necessary: (1) the factor that influences the expression of AQP7 in skeletal muscle, for example, as AQP4 expression is controlled by the influence of nerves (Jimi et al. 2000), does denervation influence the expression of AQP7? (2) The AQP7 expression of muscle cells in a physiologic condition, such as muscle cell development or regeneration. (3) The conditions of AQP7 expression in pathological skeletal muscles, such as in muscular dystrophies. The clarification of these issues may throw further light onto the detailed functional roles of the AQP7 molecule in skeletal muscles.

**Fig. 3A–D** Immunohistochemical staining of normal human muscle with anti-aquaporin 7 (anti-AQP7) antibody. The cell surface of each myofiber showed a thin layer of immunofluorescence with this antibody and no intracellular structures were stained (**A**). Myofibers immunostained with immunodepleted anti-AQP7 antibody solution showed negative immunostaining (**B**). Immunostaining with anti-AQP4 antibody in the human muscle contained both strongly stained human myofibers and weakly stained ones (**D**, *asterisks*), but the immunostaining of serial sections with anti-AQP7 antibody showed strong positive immunostaining in all human myofibers, including myofibers with *asterisks* in **D** (**C**, *asterisks*).  $\times 330$  (**A–D**). Scale bars 50  $\mu\text{m}$  (**A–D**)



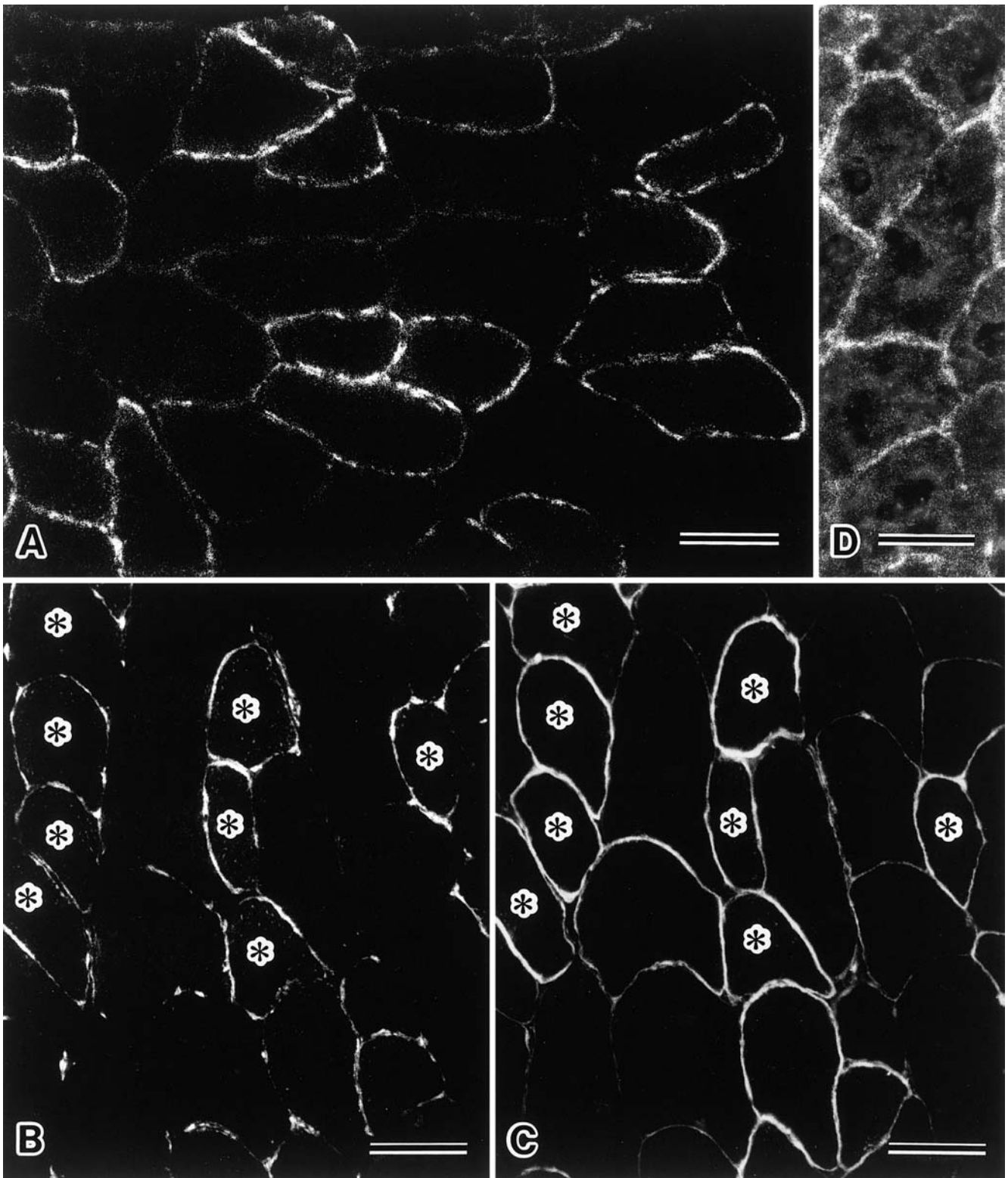


**Fig. 4A–D** In contrast to Fig. 3C, D, a positive immunoreaction with anti-AQP7 antibody in normal mouse muscle was at the surface of cross sections of myofibers, and the distribution of mouse myofibers with positive AQP7 immunostaining showed a checkerboard pattern (A, B). Positive immunostaining at the cell surface of cross-sectioned myofibers appeared to be discontinuous in mouse muscle. Serial sections of mouse skeletal muscle

immunostained with anti-AQP4 antibody (C) showed that positively immunostained mouse myofibers with anti-AQP7 antibody (B, *asterisks*) were also strongly immunostained with anti-AQP4 antibody (C, *asterisks*). Sections of normal mouse liver showed positive immunostaining with anti-AQP7 antibody at the periphery of hepatocytes (D).  $\times 330$  (A–C),  $\times 660$  (D). Scale bars 50  $\mu\text{m}$  (A–C), 25  $\mu\text{m}$  (D)

**Acknowledgements** The authors thank Mrs. Y. Ohashi, Mrs. Y. Matsuzaki and Ms. C. Tochimoto for their technical help.

## References

- Crosbie RH, Dovico SA, Flanagan JD, Chamberlain JS, Ownby CL, Campbell KP (2002) Characterization of aquaporin-4 in muscle and muscular dystrophy. *FASEB J* 16:943–949
- Frigeri A, Nicchia GP, Verbavatz JM, Valenti G, Svelto M (1998) Expression of aquaporin-4 in fast-twitch fibers of mammalian skeletal muscle. *J Clin Invest* 102:695–703
- Frigeri A, Nicchia GP, Nico B, Quondamatteo F, Herken R, Roncali L, Svelto M (2001) Aquaporin-4 deficiency in skeletal muscle and brain of dystrophic mdx mice. *FASEB J* 15:90–98
- Frigeri A, Nicchia GP, Repetto S, Bado M, Minetti C, Svelto M (2002) Altered aquaporin-4 expression in human muscular dystrophies: a common feature? *FASEB J* 16:1120–1122
- Hasegawa H, Ma T, Skach W, Matthay MA, Verkman AS (1994) Molecular cloning of a mercurial-insensitive water channel expressed in selected water-transporting tissues. *J Biol Chem* 269:5497–5500
- Hatakeyama S, Yoshida Y, Tani T, Koyama Y, Nihei K, Ohshiro K, Kamiie JI, Yaoita E, Suda T, Hatakeyama K, Yamamoto T (2001) Cloning of a new aquaporin (AQP10) abundantly expressed in duodenum and jejunum. *Biochem Biophys Res Commun* 287:814–819
- Hwang SM, Lee RH, Song JM, Yoon S, Kim YS, Lee SJ, Kang SK, Jung JS (2002) Expression of aquaporin-5 and its regulation in skeletal muscle cells. *Exp Mol Med* 34:69–74
- Inase N, Fushimi K, Ishibashi K, Uchida S, Ichioka M, Sasaki S, Marumo F (1995) Isolation of human aquaporin 3 gene. *J Biol Chem* 270:17913–17916
- Ishibashi K, Sasaki S, Fushimi K, Uchida S, Kuwahara M, Saito H, Furukawa T, Nakajima K, Yamaguchi Y, Gojobori T, Marumo F (1994) Molecular cloning and expression of a member of the aquaporin family with permeability to glycerol and urea in addition to water expressed at the basolateral membrane of kidney collecting duct cells. *Proc Natl Acad Sci U S A* 91:6269–6273
- Ishibashi K, Kuwahara M, Gu Y, Kageyama Y, Tohsaka A, Suzuki F, Marumo F, Sasaki S (1997) Cloning and functional expression of a new water channel abundantly expressed in the testis permeable to water, glycerol, and urea. *J Biol Chem* 272:20782–20786
- Ishibashi K, Yamauchi K, Kageyama Y, Saito-Ohara F, Ikeuchi T, Marumo F, Sasaki S (1998) Molecular characterization of human aquaporin-7 gene and its chromosomal mapping. *Biochim Biophys Acta* 1399:62–66
- Jimi T, Wakayama Y, Murahashi M, Shibuya S, Inoue M, Hara H, Matsuzaki Y, Uemura N (2000) Aquaporin 4: lack of mRNA expression in the rat regenerating muscle fiber under denervation. *Neurosci Lett* 291:93–96
- Koyama N, Ishibashi K, Kuwahara M, Inase N, Ichioka M, Sasaki S, Marumo F (1998) Cloning and functional expression of human aquaporin8 cDNA and analysis of its gene. *Genomics* 54:169–172
- Kuriyama H, Kawamoto S, Ishida N, Ohno I, Mita S, Matsuzawa Y, Matsubara K, Okubo K (1997) Molecular cloning and expression of a novel human aquaporin from adipose tissue with glycerol permeability. *Biochem Biophys Res Commun* 241:53–58
- Liu JW, Wakayama Y, Inoue M, Shibuya S, Kojima H, Jimi T, Oniki H (1999) Immunocytochemical studies of aquaporin 4 in the skeletal muscle of mdx mouse. *J Neurol Sci* 164:24–28
- Preston GM, Jung JS, Guggino WB, Agre P (1993) The mercury-sensitive residue at cysteine 189 in the CHIP28 water channel. *J Biol Chem* 268:17–20
- Shi LB, Verkman AS (1996) Selected cysteine point mutations confer mercurial sensitivity to the mercurial-insensitive water channel MIWC/AQP-4. *Biochemistry* 35:538–544
- Umenishi F, Verkman AS, Gropper MA (1996) Quantitative analysis of aquaporin mRNA expression in rat tissues by RNase protection assay. *DNA Cell Biol* 15:475–480
- van Hoek AN, Yang B, Kirmiz S, Brown D (1998) Freeze-fracture analysis of plasma membranes of CHO cells stably expressing aquaporins 1–5. *J Membr Biol* 165:243–254
- Wakayama Y, Jimi T, Takeda A, Misugi N, Kumagai T, Miyake S, Shibuya S (1990) Immunoreactivity of antibodies raised against synthetic peptide fragments predicted from mid portions of dystrophin cDNA. *J Neurol Sci* 97:241–250
- Wakayama Y, Kojima H, Inoue M, Murahashi M, Shibuya S, Takahashi J, Oniki H (2001) Confocal laser and immunoelectron microscopic studies of aquaporin 4 localization in normal skeletal myofiber. *Acta Myologica* 20:125–129
- Wakayama Y, Jimi T, Inoue M, Kojima H, Murahashi M, Kumagai T, Yamashita S, Hara H, Shibuya S (2002a) Reduced aquaporin 4 expression in the muscle plasma membrane of patients with Duchenne muscular dystrophy. *Arch Neurol* 59:431–437
- Wakayama Y, Jimi T, Inoue M, Kojima H, Shibuya S, Murahashi M, Hara H, Oniki H (2002b) Expression of aquaporin 3 and its localization in normal skeletal myofibers. *Histochem J* 34:331–337
- Yang B, Brown D, Verkman AS (1996) The mercurial insensitive water channel (AQP-4) forms orthogonal arrays in stably transfected Chinese hamster ovary cells. *J Biol Chem* 271:4577–4580
- Yang B, Verbavatz JM, Song Y, Vetrivel L, Manley G, Kao WM, Ma T, Verkman AS (2000) Skeletal muscle function and water permeability in aquaporin-4 deficient mice. *Am J Physiol Cell Physiol* 278:C1108–C1115